# NUMERICAL PREDICTION OF HURRICANE MOVEMENT WITH THE EQUIVALENT-BAROTROPIC MODEL[1]

*Gene E. Birchfield*

The University of Chicago

(Original manuscript received 22 August 1960; revised manuscript received 10 October 1960)

ABSTRACT

Equivalent-barotropic-model predictions of hurricane trajectories made with a 150-km grid mesh are presented. By a series of comparative tests, the results suggest that more accurate forecasts were obtained using density-weighted mean initial data than with 500-mb data. The importance of horizontal mesh size on the accuracy of the calculations is also shown.

## 1. Introduction

Commensurate with the available synoptic observations in a hurricane, and to some extent with the understanding of the dynamics of the storms, numerical models concerned with hurricane prediction until quite recently have been almost exclusively limited in purpose to the prediction of the movement with the very simplest of physical models. While ultimate improvement of the accuracy of the forecasts will result from increasing the generality of the physical model, it is the purpose of this paper to indicate by a series of comparative tests that a significant range of improvement in accuracy of trajectory prediction may exist within the framework of the equivalent-barotropic model, the simplest dynamical model.

## 2. The equivalent-barotropic model

Since numerous discussions of the equivalent-barotropic model appear in the literature (for example: Charney, 1949), only a brief description will be presented here. The vorticity equation in pressure coordinates can be written

$$\frac{\partial \zeta}{\partial t} + \boldsymbol{V}\cdot\nabla(\zeta + f) - f\frac{\partial \omega}{\partial p} - \zeta\frac{\partial \omega}{\partial p} + \omega\frac{\partial \zeta}{\partial p} + \frac{\partial \omega}{\partial x}\frac{\partial v}{\partial p} - \frac{\partial \omega}{\partial y}\frac{\partial u}{\partial p} = 0 \quad (2.1)$$

where $\zeta = (\partial v/\partial x) - (\partial u/\partial y)$ is the vertical component of vorticity, $\boldsymbol{V}$ the horizontal velocity vector, and $\omega \equiv dp/dt$. The principal assumptions involved in the equivalent-barotropic or one-parameter model are the following.

(1) The horizontal wind $\boldsymbol{V}$ can be approximated by $\boldsymbol{V} = A(p)\overline{\boldsymbol{V}}$ where $\overline{\boldsymbol{V}}$ represents a density-weighted average of $\boldsymbol{V}$ from the top to the bottom of the atmosphere; $A(p)$ is a function to be determined in some manner from the initial data.

(2) The last four terms in (2.1) for large-scale atmospheric disturbances are approximately one order of magnitude smaller than the first three terms in the equation.

(3) At the top and bottom of the atmosphere, the vertical velocity $\omega = 0$.

If, in addition to application of these assumptions, $\overline{\boldsymbol{V}}$ is replaced by the mean geostrophic wind $\overline{\boldsymbol{V}} = -(g/f)\nabla\overline{Z} \times \boldsymbol{K}$ where $\boldsymbol{K}$ is a unit vector in the $-p$ direction, and if we define $\hat{Z} \equiv \overline{A^2}\overline{Z}$, (2.1) can be reduced to the following prediction equation:

$$\frac{\partial \hat{Q}}{\partial t} = \frac{g}{f}J(\hat{Q}, \hat{Z})$$

$$\hat{Q} = \frac{g}{f}\nabla^2\hat{Z} + f \quad (2.2)$$

$$J(u, v) \equiv \frac{\partial u}{\partial x}\frac{\partial v}{\partial y} - \frac{\partial v}{\partial x}\frac{\partial u}{\partial y}.$$

Eq (2.2) is identical in form to the vorticity equation for a barotropic nondivergent atmosphere, the quantity $\hat{Q}$ (analogous to the absolute vorticity) being conserved following the horizontal motion.

The assumptions made in the equivalent-barotropic model are, at most, reasonable for prediction of large-scale atmospheric disturbances; if one must accurately predict hurricane-scale motions, these assumptions can easily be shown to be inadequate. Our interest, however, is confined to the prediction of the *movement* of the hurricane. If we make the additional assumption that, for relatively short forecast periods, the movement is to a great extent influenced by the large-scale motions near the storm and to a lesser extent by the small-scale motions, then we have some justification for use of the equivalent-barotropic model.

[1] This research was sponsored by the U. S. Weather Bureau, under Contract Number 9718 with The University of Chicago.

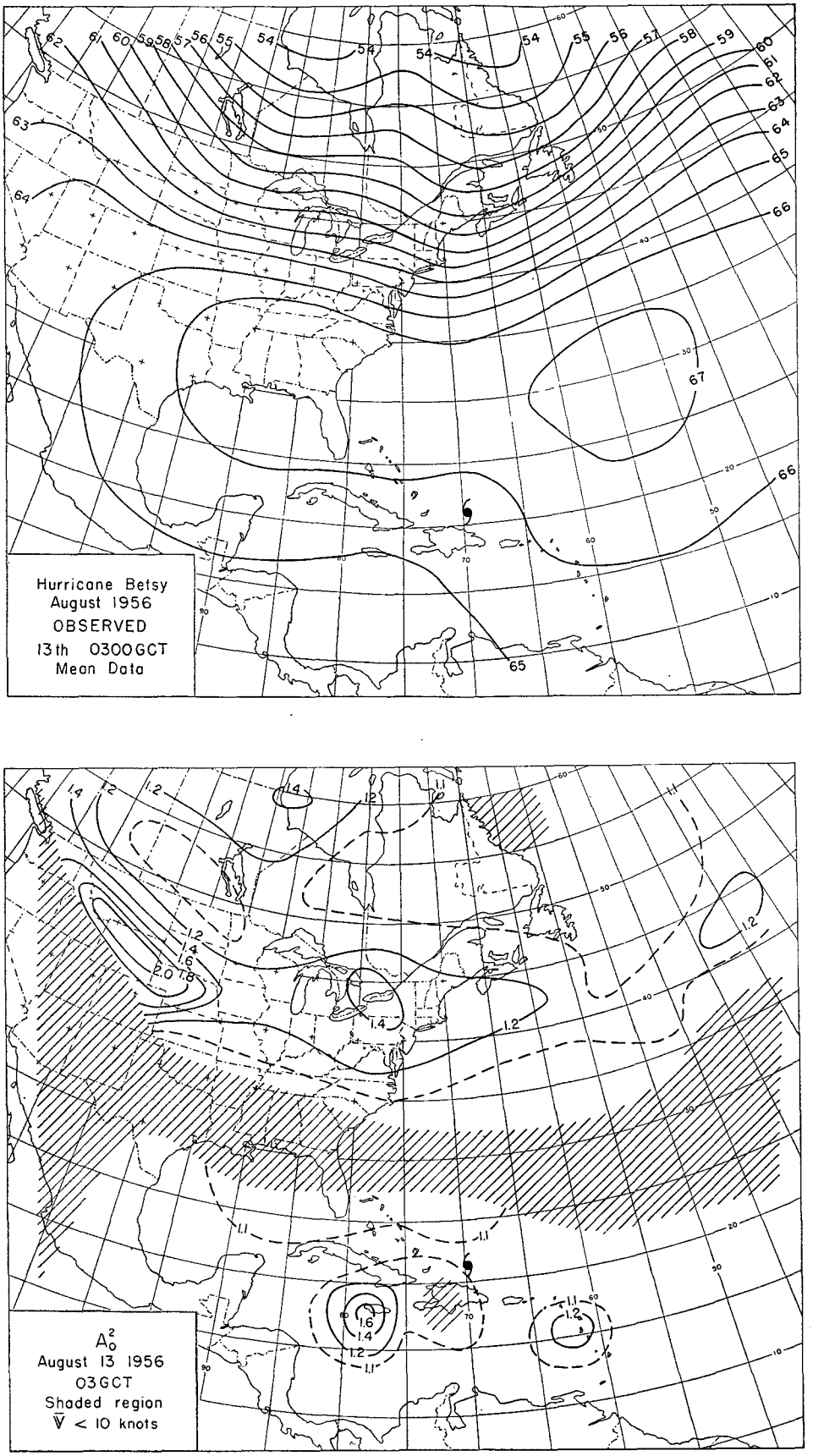


FIG. 1. Upper: mean height field, intervals of hundreds of feet. Add 10,000 ft to obtain mean height. Lower: $\overline{A_0^2}$ for the same time in units of 0.2. Shaded areas denote regions where $|\bar{V}| < 10$ mph.

### 3. The numerical model

The geographical region of integration is shown in fig. 1; the dimensions are approximately 6,300 by 7,200 km. The map base used is a Lambert conformal projection, with standard latitudes of 30 and 60 deg. The map reduction factor is 1:12,500,000. The finite-difference interval was chosen to be $\Delta S = 150$ km; a corresponding $\Delta t$ was chosen equal to $\frac{1}{2}$ hr. The grid then consists of $49 \times 43$ or 2107 points; for a forecast of 48 hr, 96 iterations are performed. The program was coded for the IBM-704, with a 32,768-word core storage and half-word logic.

Eq (2.1) are replaced by a corresponding set of finite-difference equations; centered differences are used for space and time derivatives except for the initial time step where a forward time difference is used.

To form an approximation to the initial mean wind field $\bar{V}$, data at four levels (1000, 700, 500 and 200 mb) were used. If the vertical averaging operation is defined $\overline{(\ )} \equiv (p_1 - p_0)^{-1}\int_{p_0}^{p_1}(\ )dp$ where $p_0, p_1$ represent the pressure at the top and bottom of the atmosphere respectively, a numerical approximation is found in the following way. To find a set of weight factors $\alpha_j$ such that

$$\bar{Z} = \sum_{j=0}^{3} \alpha_j Z_j, \tag{3.1}$$

we represent $Z$ by a cubic polynomial

$$Z_j = \sum_{i=0}^{3} a_i p_j{}^i. \tag{3.2}$$

If we apply the bar operator to (3.2) and equate it to (3.1), we have, after eliminating $Z_j$ with (3.2) and interchanging an order of summation,

$$\sum_{i=0}^{3}\left[\frac{1}{p_1 - p_0}\cdot\frac{p^{i+1}}{i+1}\Big|_{p_0}^{p_1} - \sum_{j=0}^{3}\alpha_j p_j{}^i\right]a_i = 0.$$

Since $a_i$ are arbitrary constants, we have four linear equations for $\alpha_j$:

$$\sum_{j=0}^{3}\alpha_j p_j{}^i - \frac{1}{p_1 - p_0}\frac{p^{i+1}}{i+1}\Big|_{p_0}^{p_1} = 0. \tag{3.3}$$

Though there is a considerable evidence that the vertical velocity may reach a maximum very high in the troposphere (see, for example, Eliassen, 1953), it seemed reasonable to impose $\omega = 0$ at 200 mb near the tropopause level; thus, $p_0$ was chosen to be 200 mb and $p_1$ was set equal to 1000 mb. The weight factors found from (3.3) are tabulated in table 1.

The function $A(p)$ was determined from the initial data by a least-squares method. Define $\boldsymbol{V}^* \equiv A(p)\bar{\boldsymbol{V}}(x, y, t)$ and let $\boldsymbol{V}(x, y, p, 0)$ represent the observed initial wind. We wish to determine the function $A(p)$ such that $I \equiv \int\int\overline{(\boldsymbol{V} - \boldsymbol{V}^*)^2}dS$ is minimized, where the bar represents integration with respect to $p$. By taking the variation with respect to $A(p)$,

$$\delta\int\int\overline{(\boldsymbol{V} - A\bar{\boldsymbol{V}})^2}dS = 2\int\int\overline{(\boldsymbol{V} - A\bar{\boldsymbol{V}})\bar{\boldsymbol{V}}\delta A}dS = 0.$$

If we interchange the horizontal and vertical limits of integration, we have

$$\int_{p_1}^{p_0}(\widetilde{\boldsymbol{V}\cdot\bar{\boldsymbol{V}}} - A(p)\widetilde{\bar{\boldsymbol{V}}^2})\delta A dp = 0,$$

$$\widetilde{(\ )} \equiv \int\int_S(\ )dS.$$

Since $\delta A$ is arbitrary between $p_1$ and $p_0$, the integrand must vanish and

$$A(p) = \widetilde{\boldsymbol{V}\cdot\bar{\boldsymbol{V}}}/\widetilde{\bar{\boldsymbol{V}}^2}.$$

The wind vector is then replaced by the geostrophic wind, and the area integral is replaced by an area-weighted sum over the grid points:

$$A(p) = \frac{\sum_{ij}\frac{g^2}{f_{ij}{}^2}(\nabla_p Z_{ij}\cdot\nabla_p\bar{Z}_{ij})}{\sum_{ij}\frac{g^2}{f_{ij}{}^2}(\nabla_p\bar{Z}_{ij})^2}$$

where $\nabla_p$ is the del operator on the map projection. Given $Z_{ij}$, $A(p)$ and $\overline{A^2}$ can then be computed for each set of initial data.

In order to provide an objective estimate of the location of the storm center during the prediction, a tracking program was incorporated into the numerical model. Only a general description is given here.

The initial coordinates of the storm are included as part of the initial data. At each time step, an interpolating polynomial is fitted to the height field adjacent to the storm. The minimum is located and its position recorded in the output data. Because of truncation errors, it frequently occurs that the profile of the vortex becomes greatly flattened out, sometimes completely disappearing during the forecast. Provision is made in the program to determine whether the vortex as such vanishes during the forecast; if this occurs, the numerical prediction is caused to terminate at the end of the current twelve-hour period.

TABLE 1. Weight factors to compute mean data.

| | |
|---|---|
| 1000 | 0.14444 |
| 700 | 0.35556 |
| 500 | 0.35556 |
| 200 | 0.14444 |

The output for each forecast consisted of the trajectory tabulation for each time step, a binary history tape of the vorticity field, contoured height and vorticity fields for the entire region of integration for 300-km grid points and a local map of height and vorticity near the storm for 150-km grid points. The grid print-outs were performed every 12 hr.

## 4. Initial data

Subjective analyses of the 1000-, 700-, 500- and 200-mb pressure levels were made for the period 13 August to 18 August 1956 (Hurricane Betsy) 0300 and 1500 GCT, by Robert W. Jones of the Department of Meteorology, The University of Chicago. Careful attention was paid to the consistency between the four levels and to the time continuity of the series (Jones, 1960).

Although the finite-difference interval used was 150 km, data were read off at 300-km grid points except in the immediate vicinity of the hurricane where 150-km data were read off. For the remaining grid points, height values were interpolated internally by the program at the outset of the calculation.

Because of the small scale of the hurricane, very large truncation errors are made at the points adjacent to the storm center. This particular storm was so small that there were only very few grid points in its circulation. In several instances, a single point (closest to the center) would have a very low value relative to the nearby grid points.

To reduce truncation error, the height values near the vortex were systematically modified by a graphical method which has been described previously by the writer (Birchfield, 1957). In summary, this consists of replacing the geostrophic height values in the storm's circulation by a stream function (with a dimensionalizing factor) obtained by integrating the gradient-wind equation.

The variation of $\overline{A^2}$, computed for each of the ten sets of initial data, was so small during the period that the mean value 1.1 was chosen as a constant for all of the forecasts.

An examination was made of the validity of the one-parameter representation of the wind field. To estimate the spatial distribution of $\overline{A^2}$, the quantity

$$A_0(p) \equiv \boldsymbol{V}\cdot\overline{\boldsymbol{V}}/\overline{\boldsymbol{V}}^2$$

was computed at each grid point for one set of data. Fig. 1 illustrates the mean height field and the corresponding field $\overline{A_0^2}$. Since $A_0$ loses its significance when $|\overline{\boldsymbol{V}}|$ is small, the areas in fig. 1 where $|\overline{\boldsymbol{V}}| < 10$ mph have been excluded by shading. Regions of large values of $\overline{A_0^2}$ indicate large vertical wind shear and corresponding horizontal temperature gradients. The large values in the lower latitudes west of the hurricane are associated with a large cyclone in the upper troposphere. It is seen that there are extensive regions where $\overline{A_0^2} < 1.1$, particularly in low latitudes.

Further information about the latitudinal variation of $A_0(p)$ and $\overline{A_0^2}$ is presented in fig. 2. Fig. 2a consists of ten hodographs along the 75th meredian for the same data shown in fig. 1. The double arrow indicates the mean wind for each point. Fig. 2b is a plot of $\overline{A_0^2}$ as a function of latitude along the 75th meredian. Fig. 2c is a plot of the quantity

$$[\overline{(\boldsymbol{V} - A(p)\overline{\boldsymbol{V}})^2}]^{\frac{1}{2}}$$

and $|\overline{\boldsymbol{V}}|$, the magnitude of the mean wind. The former quantity is a measure of the goodness of the fit of the model wind to the observed wind. Fig. 2d shows the percentage error of the wind to the observed wind. Fig. 2e is a plot of $A_0(p)$ at each of the latitudes. Plotted at the left of 2e in dots is the function $A(p)$ for the entire region.

It should be noted that the maximum percentage error occurs in low latitudes, but that in the region of maximum winds in the middle-latitude jet stream the wind approximation is reasonably good. By comparing $A_0(p)$ with $A(p)$, it is seen that in the middle and higher latitudes they are similar in shape, but in low latitudes they differ radically. This suggests that, although the equivalent-barotropic model may be a reasonable first approximation in middle latitudes, in low latitudes it may not be so satisfactory. The trajectory forecasts discussed below, however, do not appear to show greater error in lower latitudes.

## 5. Discussion of forecast results

Out of ten forecasts made, eight ran through at least 24 hr; in the remaining two, the vortex disappeared before 24 hr, as detected by the tracking program. The predicted trajectories for 0300 and 1500 GCT are illustrated in the first and second parts (from the left) of fig. 3. Dots indicate 150-km grid points.

Because of the very flat gradient near the vortex center in the graphically modified height data described above, it was difficult to insure that the initial location of the minimum height coincided with the original observed center. As a consequence, in some initial data the tracking routine recorded a different initial position of the vortex. This was rectified in the verification by displacing the 24-hr predicted position in the opposite manner to which the initial position was displaced.

If $\vec{S}$ and $\vec{S}_p$ represent the observed and predicted displacement respectively, then the vector error is defined $\vec{E}_v \equiv \vec{S}_p - \vec{S}$. The error in displacement is defined $E_s \equiv |\vec{S}_p| - |\vec{S}|$. The vector error was drawn to the corrected position from the observed position.

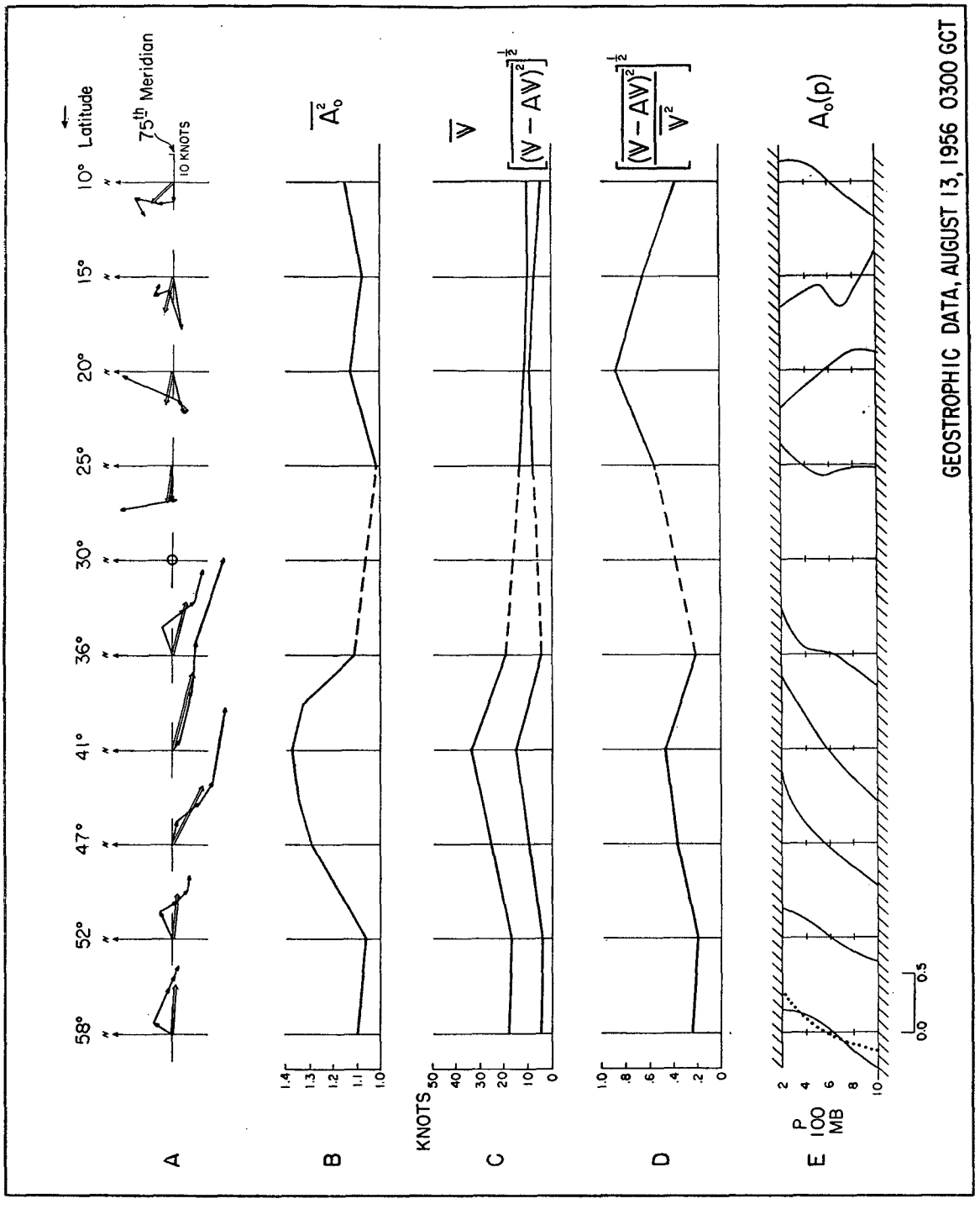


FIG. 2. (A) Hodographs along the 75th meridian. Double arrow represents the mean wind. (B) through (E) consist of the labeled quantities at the same latitudes on the 75th meridian as in (A). Dotted curve at left of (E) represents $A(p)$ for the entire region.

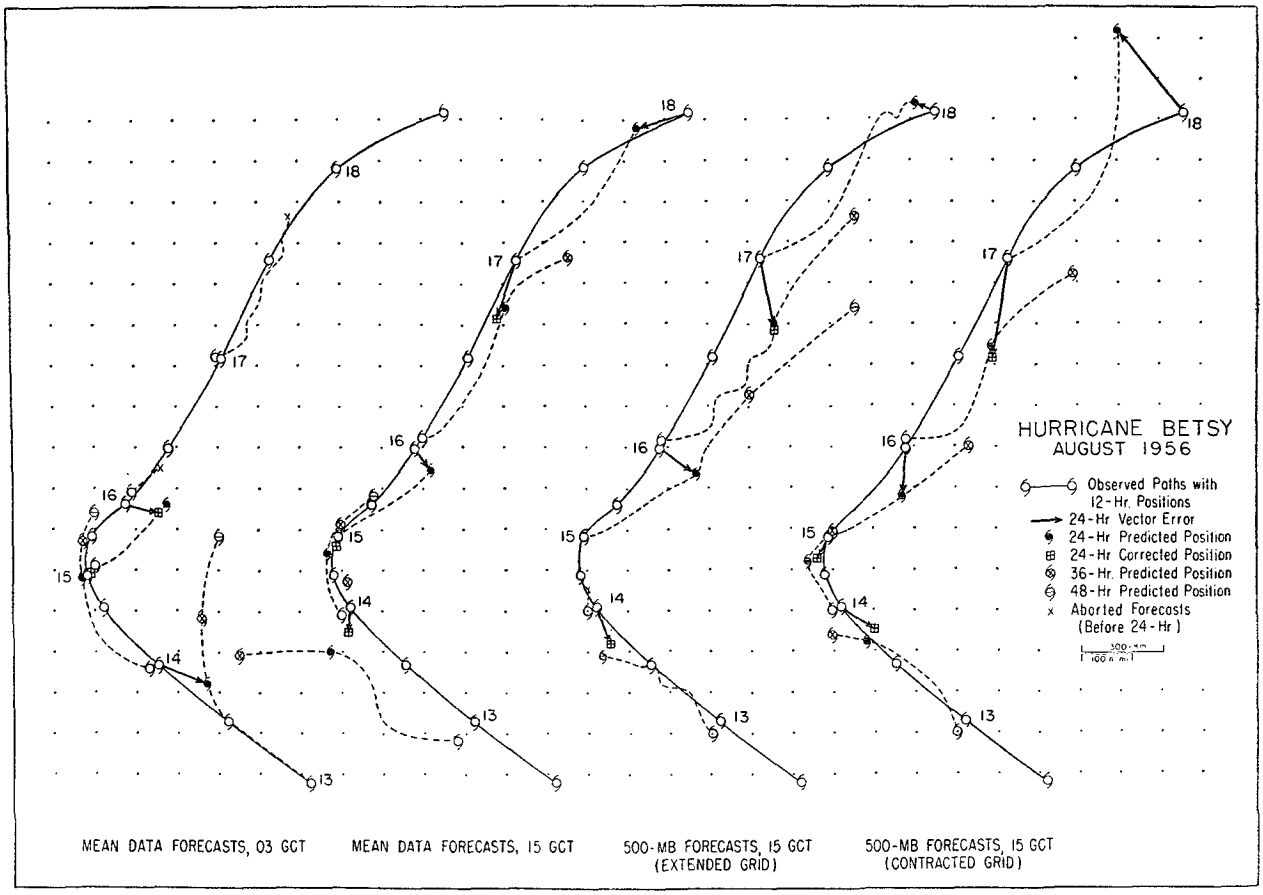


FIG. 3. Observed and predicted trajectories for three different sets of calculations.

For eight 24-hr forecasts, the mean magnitude of the vector error was 67 n. mi. The average magnitude of displacement error was 56 n. mi. It appears from fig. 3 that there is generally an under-prediction of displacement. There seems, however, to be little tendency for systematic deflection to the left or right of the observed path. The recurvature of the hurricane has been very well predicted from the 14th both from 0300 GCT and 1500 GCT.

To investigate the effect of variations of $\overline{A^2}$ on the predicted trajectory, forecasts for two sets of initial data were made by using $\overline{A^2} = 1.0$ and $\overline{A^2} = 1.2$. For both sets of data, the only significant difference was a reduction in the computed displacement for the lower value of $\overline{A^2}$ and an increase in displacement for the higher value, compared to the chosen value $\overline{A^2} = 1.1$.

In general, these eight 24-hr forecasts can be considered good forecasts relative to other numerical predictions; in particular, they are a great improvement over those made previously for Hurricane Betsy by the writer (Birchfield, 1960). These predictions employed essentially the same physical model — the equivalent-barotropic model. Because of the significant improvement, a closer examination of the two numerical models was made. The differences between the two models were found to be of two types: differences in the initial data, and differences in the finite-difference model.

In the previous model, 500-mb initial data were used instead of mean data. For the new forecasts, new and independent analyses of the storm situation have been used for the initial data. Also, in the earlier predictions, the height data near the vortex were not modified as in the mean-data forecasts.

The principal difference in the finite-difference model was the use in the earlier one of a two-grid scheme where the 150-km grid was contracted to a region covering only the neighborhood of the vortex; the remaining part of the region of integration was covered by a 300-km grid. In the new prediction, a 150-km net extended over the entire forecast region.

It is important to determine the relative usefulness of mean initial data *versus* 500-mb initial data. To clarify this question and to determine the significance of the contracted grid *versus* the extended grid, two supplementary sets of forecasts were made. First: to eliminate the effect of the difference in analyses,

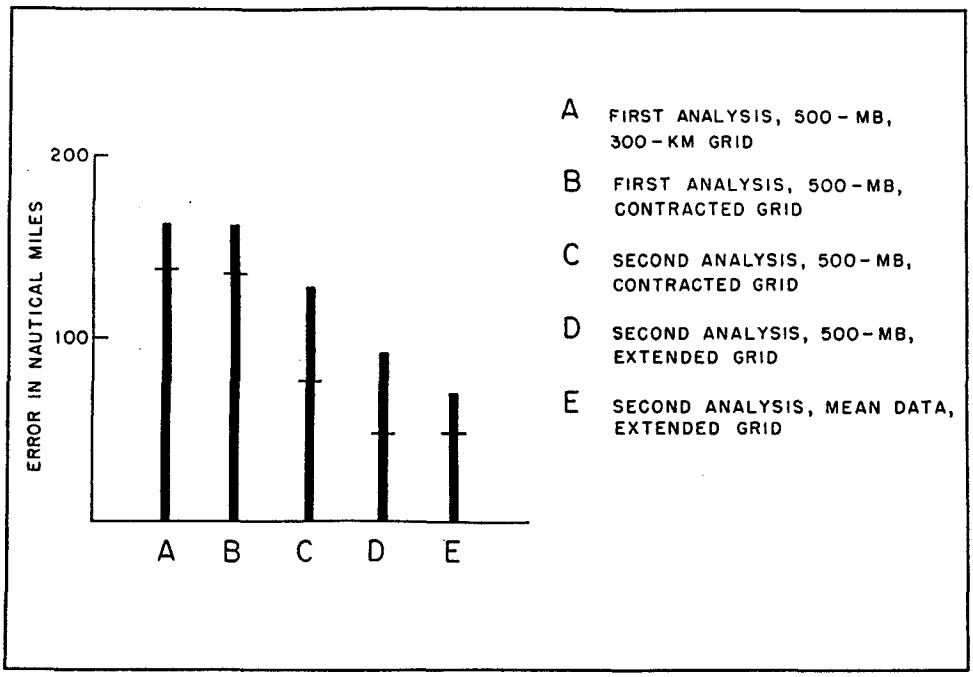


FIG. 4. Mean magnitude of the vector error, $E_v$; horizontal bar represents the mean magnitude of the displacement error, $E_s$. "Contracted-grid" forecasts are those made with a local 150-km grid over the storm, superimposed on a 300-km grid covering the entire region. "Extended-grid" forecasts are those made with a 150-km grid covering the entire region.

forecasts using 500-mb data from the new analysis were made with the contracted grid; these could then then be compared with the original Betsy forecasts. Second: a set of supplementary predictions was made using the new 500-mb data with the extended-grid forecasts. The supplementary forecasts were for only the 1500 GCT data, 13 to 17 August; 24-hr predictions were made.

The third and fourth parts of fig. 3 illustrate the predicted trajectories for the 500-mb extended-grid forecasts and for the 500-mb contracted-grid forecasts, respectively. By comparing visually the mean-data forecasts with the 500-mb forecasts, it is apparent that there is a reasonable improvement in the former. The mean-data predictions tend to lie more nearly along the observed path than the 500-mb forecasts. Again, the visual comparison of the 500-mb extended-grid forecasts with the contracted-grid forecasts indicates an improvement in the former.

A comparison of the two statistics $E_v$ and $E_s$ among these two supplementary calculations, the old Betsy forecasts and the mean-data forecasts is shown in fig. 4. Here, there is a remarkable difference among the sets. The comparison of the old analysis with the new analysis (B with C) indicates that a large part of the error in the old 500-mb forecasts was due to analysis of the initial data. It should be remembered, however, that the data from the old analyses were not graphically modified near the vortex as were the new analyses. Comparisons among C, D and E are consistent with the conclusions drawn from the trajectories in fig. 3.

As a further control on these comparisons, 300-km grid forecasts made for the corresponding five Betsy forecasts from the first analysis of 500-mb data have been included as part A of fig. 4. In the previous report by the writer (Birchfield, 1960), it was concluded from a larger sample (11 cases, three storms) that there was an improvement in the 150-km contracted grid forecasts over 300-km grid forecasts. That this does not appear in comparing A with B in fig. 4 may be regarded as a further indication of the importance of analysis on prediction error.

The second analyses of Hurricane Betsy, which have been used in the above comparisons of forecasts, have also been used as initial data by Kasahara (1959) in a series of hurricane-trajectory predictions using a two-level baroclinic steering-flow model. Very briefly, the steering-flow technique consists in removing the circulation of the hurricane and essentially performing a trajectory calculation in the residual or steering flow. The initial data for the two levels are determined by taking a properly weighted average of the four levels of data available.

From the report by Kasahara cited above, for the eight 24-hr steering-flow predictions corresponding to the eight mean-data forecasts presented here, the mean magnitude of vector error $E_v$ and the mean magnitude of the displacement $E_s$ were computed to be 100 and 64 n. mi. respectively. These are to be com-

pared with $E_v = 67$ n. mi., and with $E_s = 56$ n. mi. for the mean-data forecasts. It is seen that the error in prediction of displacement as represented by $E_s$ is essentially the same for the two sets of forecasts; the larger difference in $E_v$ represents a difference in error of the predicted *direction* of movement. From comparison of fig. 5 of the Kasahara report with fig. 3 here, it is seen that the steering-flow model's systematic predicted deflection to the right of the observed path is considerably reduced in the mean-data forecasts. This raises the question of the role of the coupling between the vortex circulation and the larger-scale environment on the movement of the storm. In the steering-flow model, the influence of the storm's circulation is essentially removed. In the mean-data model, though very crudely represented, the vortex circulation is able to influence the environment. It can be shown very simply that, if the hurricane and the adjacent subtropical anticyclone to the east are treated as an isolated system (for example, if they are replaced by two vortex filaments), by reducing the circulation of the hurricane, then, the path of the vortex is deviated to the right. Whether or not this can easily be extended to the total continuous field, the data show some indication of the influence of the coupling between the hurricane vortex and its environment.

## 6. Conclusions

From the comparisons of the equivalent-barotropic forecasts presented here, the following conclusions are put forth. There is an indication that density-weighted mean data are more nearly representative of a nondivergent atmosphere than are 500-mb data. The mean-data trajectory forecasts show an improvement in the direction of movement compared to the 500-mb forecasts. The use of a finer grid net makes a significant improvement in the hurricane trajectory prediction. The use of a contracted fine grid in the neighborhood of the storm yields a definite improvement over forecasts made with a 300-km grid (Birchfield, 1960), but a still greater improvement is made by extending the fine grid (150 km) over the entire forecast region. Finally, from comparison with steering-flow forecasts, there is some indication that the smaller-scale circulation of the hurricane may exert a distinct influence on the movement of the storm.

## 8. Acknowledgments

The writer expresses his thanks to Dr. Akira Kasahara for many discussions and to Mr. Richard Peterson for assistance in hand calculations. To Professor George W. Platzman, the writer expresses his appreciation for helpful discussions and for his reading of the manuscript.

## REFERENCES

Birchfield, G. E., 1957: *Numerical prediction of hurricane movement with the use of a fine grid.* Univ. Chicago, Dept. Meteor., 14 pp.

——, 1960: Numerical prediction of hurricane movement with the use of a fine grid. *J. Meteor.*, **17**, 406–414.

Charney, J. G., 1948: On the scale of atmospheric motions. *Geofys. Publ.*, **17**, No. 2, 17 pp.

——, 1949: On a physical basis for numerical prediction of large-scale motions in the atmosphere. *J. Meteor.*, **6**, 371–385.

Eliassen, A., 1953: Computation of vertical motion and vorticity budget in a blocking situation. *Tellus*, **5**, 196–206.

Jones, R. W., 1960: The tracking of Hurricane Audrey 1957 by numerical prediction. *J. Meteor*, **18**, 127–138.

Kasahara, A., 1960: The numerical prediction of hurricane movement with a two-level baroclinic model. *J. Meteor.*, **17**, 357–370.